DOI: 10.1002/anie.200904190

# Concerted Spin Crossover and Symmetry Breaking Yield Three Thermally and One Light-Induced Crystallographic Phases of a Molecular Material**

*Nicolas Bréfuel , Hiroshi Watanabe, Loic Toupet, Jérémy Come, Naohide Matsumoto, Eric Collet,* Koichiro Tanaka, and Jean-Pierre Tuchagues**

Among switchable molecular materials, $Fe^{II}$ spin-crossover (SC) complexes have been widely studied over the last decades.[1] Their reversible low-spin (LS)$\rightleftharpoons$high-spin (HS) switching triggered by a change in temperature or pressure, or by light irradiation, has attracted much interest for both basic scientific understanding and potential technological applications in information storage or visual displays.[2,3] In these materials, the coexistence of short- and long-range interactions between molecules yields cooperative effects such as hysteresis and/or two-step transitions. Usually, the SC phenomenon is isostructural, but in a few cases symmetry breaking occurs in the LS phase, alongside intermolecular reorganization.[4,5] Few examples of mononuclear molecular materials that undergo two-step SC associated with intermolecular reorganization in the broken-symmetry phase, the so-called intermediate (INT) phase, involving fractional population of the HS state, have been reported.[6,7] To date, the INT phase has been fully described only in very few cases by diffraction techniques, which evidenced HS–LS[8,9] or LS–HS–LS[10] long- or short-range ordering.[6] Over the last ten years, we have investigated supramolecular $Fe^{II}$ SC materials including imidazolyl groups.[5,8,9,11] In view of the first-order SC evidenced in $[Fe^{II}H_2L^{2Me}](ClO_4)_2$,[5] where $H_2L^{2Me}$ denotes the acyclic hexadentate $N_6$ Schiff base bis[N-(2-methylimidazol-4-yl)methylidene-3-aminopropyl]ethylenediamine, the new SC material $[Fe^{II}H_2L^{2Me}](PF_6)_2$, **1** has been synthesized. Here we report on its two rare types of behavior: long-range LS–HS–HS–LS ordering in the INT phase, and structural symmetry breaking in the LS phase. In addition, another symmetry-breaking process occurs on generating the photoinduced HS phase (PIHS): in the emerging field of photoinduced phase transitions,[12] this result opens a new subject of debate, that is, the possibility of reaching different types of false ground states through light irradiation.

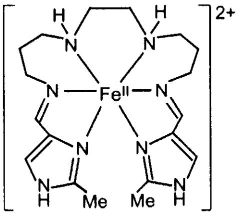

**1**

Figure 1 shows the thermal variation of the $\chi_M T$ product of **1** ($\chi_M$ is the molar magnetic susceptibility), in the cooling and warming modes, evidencing a two-step SC process. The

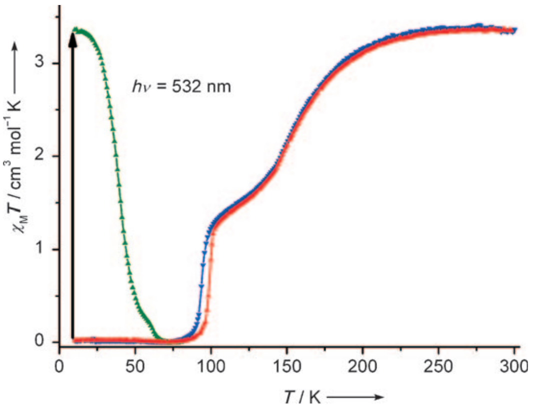

*Figure 1.* Temperature dependence of $\chi_M T$ in the 10–300 K range for **1** measured first on cooling (▼)and then on warming mode (▲), at 1 K min$^{-1}$ sweeping rate; (▲) indicates the temperature dependence of $\chi_M T$ at the same sweep rate after irradiating the sample at 10 K with a 532 nm laser.

---

[*] Dr. L. Toupet, Prof. E. Collet
Institut de Physique de Rennes, UMR CNRS 6251
Université Rennes 1, 263 av. Général Leclerc
35042 Rennes cedex (France)
Fax: (+33) 223-236717
E-mail: eric.collet@univ-rennes1.fr
Homepage: http://www.ipr.univ-rennes1.fr/php/detailmembre.php?who=342&lg=EN
Dr. N. Bréfuel ,[+] J. Come, Prof. J.-P. Tuchagues
CNRS; LCC (Laboratoire de Chimie de Coordination)
205 route de Narbonne, 31077 Toulouse (France)
and
Université de Toulouse; UPS, INPT; LCC
F-31077 Toulouse (France)
Fax: (+33) 561-553003
E-mail: jean-pierre.tuchagues@lcc-toulouse.fr
Dr. N. Bréfuel ,[+] Prof. N. Matsumoto
Department of Chemistry, Kumamoto University (Japan)
H. Watanabe, Prof. K. Tanaka
Department of Physics, Kyoto University (Japan)
and
Institute for Integrated Cell-Material Sciences
Kyoto University (Japan)

[+] Present address: Laboratoire National des Champs Magnétiques Intenses, UPR 3228, 25 Rue des Martyrs, 38042 Grenoble cedex 9 (France)

[**] This work was supported by Grants in Aid for Scientific Research (No. 16205010) from the Ministry of Education, Science, Sports, and Culture (Japan), Grants in Aid for Creative Scientific Research Program (No. 18GS0208) from the Ministry of Education, Science, Sports, and Culture (Japan), the Institut Universitaire de France, and a Grant "CREATE Ultimate" No. 4146 from Région Bretagne, France. N.B. is grateful to the JSPS for providing a Foreign Postdoctoral Fellowship.

$\chi_M T$ value is about 3.4 $\text{cm}^3\,\text{mol}^{-1}\,\text{K}$ at 300 K (HS phase) and continuously decreases to reach a pseudoplateau with a width of about 30 K centered at about 120 K, where $\chi_M T \approx 1.5\ \text{cm}^3\,\text{mol}^{-1}\,\text{K}$, the value expected for an approximately 50 % distribution of the HS and LS states (INT phase). The $\text{INT}\rightleftharpoons\text{LS}$ step centered around 97 K shows a thermal hysteresis loop of 6 K width, characteristic of a first-order transition.

When **1** was irradiated with green continuous-wave light (532 nm, 1 $\text{mW}\,\text{m}^{-2}$), a light-induced excited spin-state trapping effect (LIESST)[13] was clearly observed. The $\chi_M T$ product increased from an initial value of 0.02 $\text{cm}^3\,\text{mol}^{-1}\,\text{K}$ to a saturation regime at 3.4 $\text{cm}^3\,\text{mol}^{-1}\,\text{K}$ over one hour, which indicates quantitative photoconversion from the LS to a PIHS state. When irradiation was stopped, two relaxation steps were observed on increasing $T$ (ca. 1 $\text{K}\,\text{min}^{-1}$): an abrupt drop of $\chi_M T$ to about 0.5 $\text{cm}^3\,\text{mol}^{-1}\,\text{K}$ at 50 K is followed by a slower decrease up to 73 K, where the LS state is fully reached. This behavior was confirmed on different samples.

The crystal structures of **1** were determined by single-crystal X-ray diffraction[14] at 250 K (HS), 110 K [(INT ($^1\!/_2$HS + $^1\!/_2$LS)], and 80 K (LS). The nature of the photoinduced HS state at 15 K (PIHS) was also investigated by X-ray diffraction after laser excitation at 532 nm. The structural determinations showed acentric space groups with identical $[\text{Fe}^{\text{II}}\text{H}_2\text{L}^{2-\text{Me}}]^{2+}$ complex cations in which $\text{Fe}^{\text{II}}$ assumes an octahedral coordination environment including the six N donors of the hexadentate ligand, two Fe–N(imine), two Fe–N(amine), and two Fe–N(imidazolyl). Figure 2a illustrates how $\text{H}_2\text{L}^{2\text{Me}}$ wraps the $\text{Fe}^{\text{II}}$ metal center to yield the $[\text{Fe}^{\text{II}}\text{H}_2\text{L}^{2\text{Me}}]^{2+}$ cation.

The prominent features of the 250 K structure[14] (HS state) result from location of the iron center on a twofold symmetry axis. In the $P22_12_1$ ($Z=2$) space group,[15] the asymmetric unit is made of half a $[\text{Fe}^{\text{II}}\text{H}_2\text{L}^{2\text{Me}}]^{2+}$ cation and one $\text{PF}_6^-$ anion. The average bond length ($\langle\text{Fe–N}\rangle = 2.190$ Å) is typical of an HS $\text{Fe}^{\text{II}}$ site with six N donors.[1] As shown in Figure 2a, the crystal structure is made of cation layers and anion layers in the *ab* plane alternating along the *c* axis, alongside one another and connected through hydrogen bonds.

The X-ray data clearly indicate ordering of spin-states among the $\text{Fe}^{\text{II}}$ sites in the INT phase. The associated doubling of the crystalline *c* axis is characterized by the appearance of numerous, but weak, Bragg reflections (Figure 3) in the 97–142 K temperature range. In addition, the space group of the INT phase decreases to the nonisomorphic monoclinic subgroup $P2_1$.[14] We could not detect significant deviations of the $\beta$ angles from 90°, possibly because of domain formation, which may be associated with the resulting small decrease in crystal quality.[16]

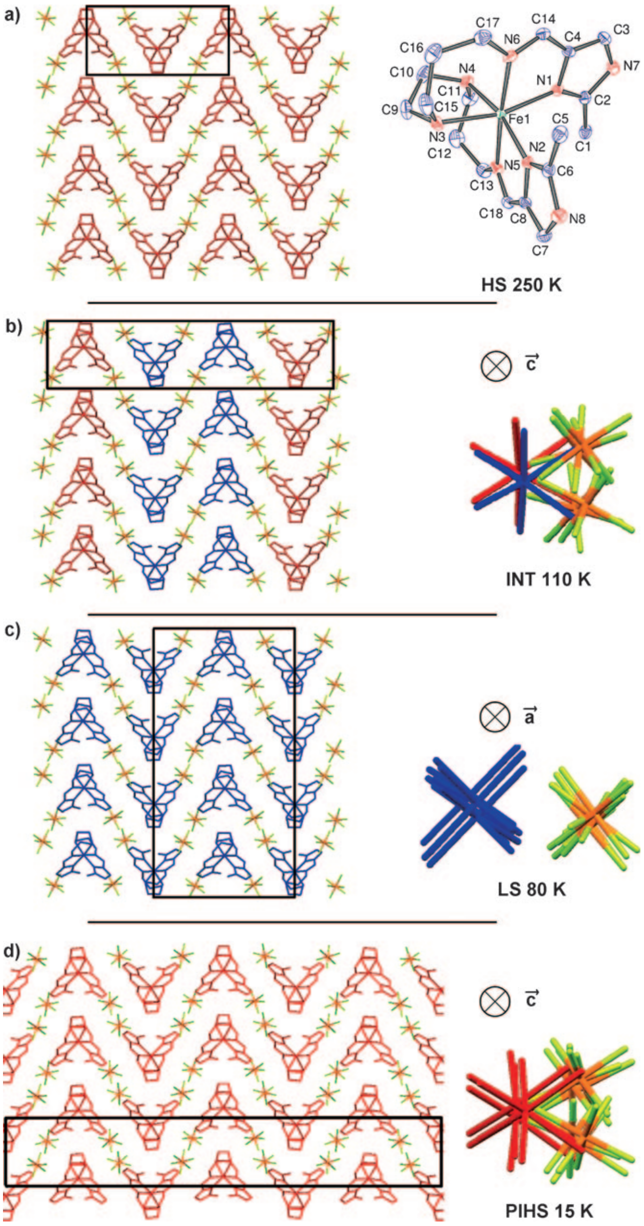

***Figure 2.*** a) Projection of the crystal packing in the HS phase of **1** at 250 K, in the *ac* plane and ORTEP of the cation with atom numbering scheme. H atoms are omitted for clarity, and thermal ellipsoids are drawn at 50 % probability. Similar projections in the *ac* plane are shown for the INT phase (b) with HS (blue) and LS (red) sites, for the LS phase (c), and for the photoinduced HS phase at 15 K (d). Additional projections along the multiplied crystal axes on the right show the motions of the ions.

There are two nonequivalent cation sites (four per unit cell) in the INT phase (Figure 2b). One is mainly HS ($\langle\text{Fe1–N}\rangle = 2.13(1)$ Å), and the other one mainly LS ($\langle\text{Fe2–N}\rangle = 2.04(1)$ Å). Noteworthily, the $\langle\text{Fe1–N}\rangle$ distance is shorter than the $\langle\text{Fe(HS)–N}\rangle$ distance at 250 K (2.190 Å) while the $\langle\text{Fe2–N}\rangle$ distance is longer than $\langle\text{Fe(LS)–N}\rangle$ distance at 80 K (2.012 Å). This suggests that the ordering does not correspond to 100 % of HS (respectively 100 % of LS) and 0 % of LS (respectively 0 % of HS) at site 1 (respectively 2), as is often observed in this type of symmetry-breaking phase transition associated with ordering phenomena.[7] The bond lengths, intermediate between those of the LS and HS states, allow a rough estimate of the HS fraction on sites 1 (2) to be 75 (25) %. As clearly observed in Figure 2b, this particular packing allows structural reorganization through displacement and collective molecular rotation within each layer, and out of phase from one layer to another. The ordering in the INT phase results in an LS–HS–HS–LS pattern, in which two

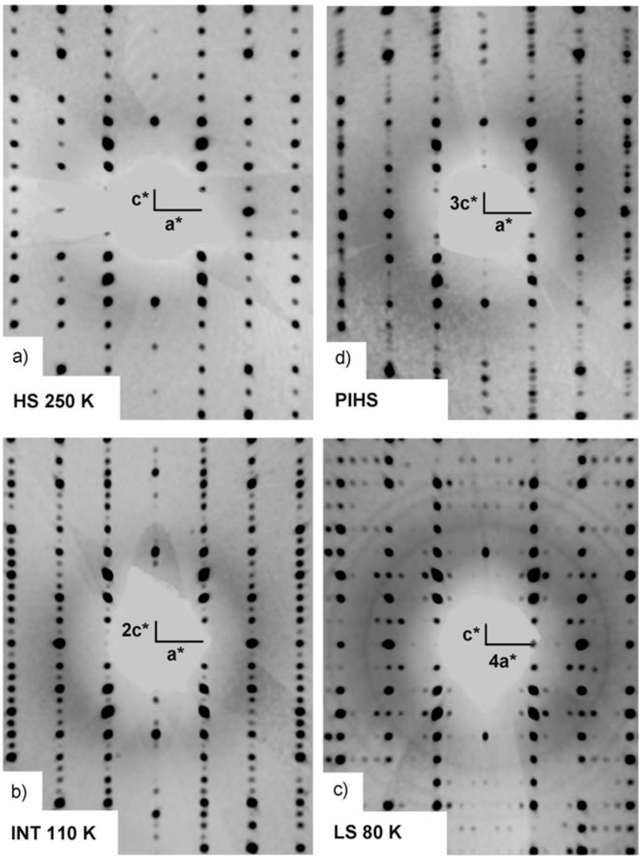

*Figure 3.* Reconstructed diffracted intensity in the $a^*c^*$ reciprocal plane. With respect to the HS reciprocal lattice at 250 K, new peaks appear at $l+1/2$ in the INT phase, at $h+1/4$, $+1/2$, $+3/4$ in the LS phase, and at $l+1/3$, $+2/3$ in the PIHS phase.

adjacent HS cation layers alternate along the *c* axis with two adjacent LS cation layers.

Such ordering phenomena have been observed in different SC systems with different types of intermediate states (HS–LS, HS–LS–LS),[7,10] and result from competition between different intrasublattice ferromagnetic-like interactions and intersublattice antiferromagnetic-like interactions.[17] These phenomena were recently discussed on the basis of the universal Landau theory of phase transitions:[18] the ordering is associated with the symmetry-breaking order parameter *y* characterizing the difference in HS population of the two sublattices $y=(\gamma_{HS1}-\gamma_{HS2})$,[18] and in the present case $y\approx 0.5$.

Below 97 K, another structure appears in the $P2_12_12_1$ space group,[14] corresponding to the LS phase, in which the unit cell has changed to (4*a*,*b*,*c*) (Figure 3). The LS structure (Figure 2c) includes two independent LS cations (Fe1 and Fe2 sites) per unit cell: $\langle \mathrm{Fe1{-}N}\rangle = 2.012$ Å $= \langle \mathrm{Fe2{-}N}\rangle$ are typical of LS $\mathrm{Fe^{II}}$. Because of symmetry breaking, the cations are no longer located on a twofold symmetry axis: a related distortion accompanied with slight tilts and displacements of the ions occurs (Figure 2c).

The present sequence of phases $P222_12_1$ (HS), $P2_1$ ($^1\!/_2$HS + $^1\!/_2$LS), $P2_12_12_1$ (LS) is therefore not “re-entrant”, and differs significantly from the already reported materials exhibiting an intermediate ordered phase[7–10] for which the LS and HS structures are isostructural. In addition, the different translation symmetries (*a*,*b*,2*c*) and (4*a*,*b*,*c*) forbid any group/subgroup relation between the INT and LS phases. This reconstructive phase transition[19] must be a first-order process, in good agreement with the thermal hysteresis observed around 97 K.

A novel structural reorganization occurs on generation of the photoinduced HS state by photoexcitation at 532 nm. The translational symmetry of this PIHS state is different from those of the HS, INT, and LS phases with an (*a*,*b*,3*c*) unit cell (Figure 3). The $P222_12_1$ space group of the PIHS phase[14] is an isomorphic subgroup of lower index of the HS phase.[16] The PIHS structure includes two independent HS complex cations per unit cell (Figure 2d), one of which is located on a twofold symmetry axis (the asymmetric unit includes $\{[\mathrm{Fe^{II}H_2L^{2-Me}}]^{2+}\}/2$). The average Fe−N bond lengths of both $\mathrm{Fe^{II}}$ sites ($\langle \mathrm{Fe1{-}N}\rangle = 2.17(1)$, $\langle \mathrm{Fe2{-}N}\rangle = 2.18(1)$ Å) are typical of HS $\mathrm{Fe^{II}}$, but the molecular distortion or rotation concerns only the layers which are not located on the twofold symmetry axis (Figure 2d). The symmetry breaking occurring in this PIHS state (triple *c* axis) also involves rotations and displacements of the ions. To our knowledge this is the first case of photoinduced spin crossover involving symmetry breaking.

The existence of different competing ground states or false ground states is a topic of current interest,[12] especially in molecular solids and in the emerging field of photoinduced phase transitions. In this respect, if the HS fraction could be stabilized between 250 and 15 K, a phase transition related to the symmetry breaking (due to ion reorganization) would occur, with change of lattice from (*a*,*b*,*c*) to (*a*,*b*,3*c*). However, temperature balances the relative stability of the different phases, and the LS phase is the true ground state. The unusual bistability of SC compounds allows a metastable HS state to be generated by light irradiation at low temperature. It is demonstrated here that this false HS ground state, otherwise inaccessible under thermal equilibrium conditions, has a symmetry different from that of the HS phase stable at high temperature.

These results clearly indicate exceptionally strong coupling between the electronic and structural degrees of freedom of **1**. The occurrence of four different phases with different symmetries, schematically shown in the table-of-contents figure, is unique and should be related to the strong intermolecular interactions and to the specific packing of anion and cation layers. The outstanding result gained from this study is revealing that light allows another type of false ground state to be reached through symmetry breaking, owing to the LIESST effect.

## Experimental Section

The $\mathrm{H_2L^{2Me}}$ ligand was prepared as previously described[5] and was deoxygenated prior to reaction with iron(II), which was carried out in a purified nitrogen atmosphere inside a glove box. **1** was obtained as dark-orange crystals as follows: a solution of $\mathrm{Fe^{II}Cl_2{\cdot}4\,H_2O}$ (0.198 g, 1 mmol) in ethanol (5 mL) was added to a solution of $\mathrm{H_2L^{2Me}}$

(1 mmol) in ethanol (10 mL) with stirring and heating (ca. 45–50 °C). After 30 min, a solution of $NaPF_6$ (0.340 g, 2 mmol) in ethanol (10 mL) was poured drop by drop into the reaction mixture. The mixture was stirred and heated for a further 1 h and filtered. The filtrate was allowed to stand for several days, and the orange crystals that formed were collected by filtration. X-ray quality dark orange crystals were obtained in 75 % yield (0.530 g) Elemental analysis (%) calcd for **1** ($FeC_{18}H_{30}N_8P_2F_{12}$, 704.3 $g\,mol^{-1}$): C 30.70, H 4.29, N 15.91; found: C 30.48, H 4.42, N 16.05, IR (KBr): $\nu = 1630$ ($\nu_{C=N}$), 843 $cm^{-1}$ ($\nu_{PF_6}$).

Received: July 28, 2009

**Keywords:** iron · magnetic properties · N ligands · phase transitions · spin crossover

---

[1] P. Gütlich, H. A. Goodwin, *Top. Curr. Chem.* **2004**, *233*, 1 – 47.

[2] O. Kahn, C. J. Martinez, *Science* **1998**, *279*, 44 – 48.

[3] J.-F. Létard, P. Guionneau, L. Goux-Capes, *Top. Curr. Chem.* **2004**, *235*, 221 – 249.

[4] J.-F. Létard, P. Guionneau, E. Codjovi, O. Lavastre, G. Bravic, D. Chasseau, O. Kahn, *J. Am. Chem. Soc.* **1997**, *119*, 10861 – 10862.

[5] N. Bréfuel, S. Imatomi, H. Torigoe, H. Hagiwara, S. Shova, J.-F. Meunier, S. Bonhommeau, J.-P. Tuchagues, N. Matsumoto, *Inorg. Chem.* **2006**, *45*, 8126 – 8135.

[6] S. Neville, B. Leita, G. Halder, C. Kepert, B. Moubaraki, J.-F. Létard, K. S. Murray, *Chem. Eur. J.* **2008**, *14*, 10123 – 10133.

[7] D. Chernyshov, M. Hostettler, K. W. Törnroos, H.-B. Bürgi, *Angew. Chem.* **2003**, *115*, 3955 – 3960; *Angew. Chem. Int. Ed.* **2003**, *42*, 3825 – 3830.

[8] D. Boinnard, A. Bousseksou, A. Dworkin, J.-M. Savariault, F. Varret, J.-P. Tuchagues, *Inorg. Chem.* **1994**, *33*, 271 – 281.

[9] M. Yamada, H. Hagiwara, H. Torigoe, N. Matsumoto, M. Kojima, F. Dahan, J.-P. Tuchagues, N. Re, S. Iijima, *Chem. Eur. J.* **2006**, *12*, 4536 – 4549; M. Yamada, M. Ooidemizu, Y. Ikuta, S. Osa, N. Matsumoto, S. Iijima, M. Kojima, F. Dahan, J.-P. Tuchagues, *Inorg. Chem.* **2003**, *42*, 8406 – 8416.

[10] S. Bonnet, M. A. Siegler, J. S. Costa, G. Molnár, A. Bousseksou, A. L. Spek, P. Gamez, J. Reedijk, *Chem. Commun.* **2008**, 5619 – 5621.

[11] Y. Sunatsuki, Y. Ikuta, N. Matsumoto, H. Ohta, M. Kojima, S. Iijima, S. Hayami, Y. Maeda, S. Kaizaki, F. Dahan, J.-P. Tuchagues, *Angew. Chem.* **2003**, *115*, 1652 – 1656; *Angew. Chem. Int. Ed.* **2003**, *42*, 1614 – 1618.

[12] K. Nasu in *Photoinduced phase transitions*, World Scientist, Singapore, **2004**.

[13] S. Decurtins, P. Gütlich, C. P. Kohler, H. Spiering, A. Hauser, *Chem. Phys. Lett.* **1984**, *105*, 1 – 4.

[14] X-ray diffraction experiments were performed on single crystals with an Xcalibur 3 four-circle diffractometer (Oxford Diffraction). We used an Oxford Cryosystems nitrogen-flow cryostat for measurements down to 80 K, and an Oxford Diffraction Helijet helium-flow cryostat for measurements at 15 K. The unit-cell parameters and data reduction were obtained with the CrysAlis software from Oxford Diffraction. The structures were solved by direct methods (SIR-97) and refined against $F^2$ by full-matrix least-squares techniques (SHELXL-97) with anisotropic displacement parameters for non-hydrogen atoms (for details, see supplementary crystallographic data). Crystal data collection and refinement parameters: **1**-250 K: $Mo_{K\alpha}$ radiation ($\lambda = 0.71073$ Å), $C_{18}H_{30}N_8P_2F_6Fe$, $M_r = 704.27$, crystal dimensions $0.20 \times 0.10 \times 0.10$ mm, orthorhombic, space group $P22_12_1$, $a = 8.405(1)$, $b = 9.469(2)$, $c = 17.399(3)$ Å, $V = 1384.7(4)$ Å$^3$, $Z$ (cations/unit cell) = 2, $\rho_{cald} = 1.689\ g\,cm^{-3}$, $\mu = 0.767\ mm^{-1}$, 21628 reflections collected, 4094 independent reflections, $wR$(all data) = 0.075, $R$(all data) = 0.042; **1**-110 K: monoclinic, space group $P2_1$, $a = 8.185(1)$, $b = 9.390(8)$, $c = 35.543(2)$ Å, $\beta = 90.011(7)°$, $V = 2655(2)$ Å$^3$, $Z$ (cations/unit cell) = 4, $\rho_{cald} = 1.762\ g\,cm^{-3}$, $\mu = 0.800\ mm^{-1}$, 64948 reflections collected, 11446 independent reflections, $wR$(all data) = 0.13, $R$(all data) = 0.13; **1**-80 K: orthorhombic, space group $P22_12_1$, $a = 32.532(3)$, $b = 9.424(1)$, $c = 17.054(1)$ Å, $V = 5228.5(8)$ Å$^3$, $Z$ (cations/unit cell) = 8, $\rho_{cald} = 1.789\ g\,cm^{-3}$, $\mu = 0.813\ mm^{-1}$, 123685 reflections collected, 11341 independent reflections, $wR$(all data) = 0.051, $R$(all data) = 0.042; **1**-15 K: orthorhombic, space group $P22_12_1$, $a = 8.226(2)$, $b = 9.330(1)$, $c = 52.20(1)$ Å, $V = 4006(4)$ Å$^3$, $Z$ (cations/unit cell) = 8, $\rho_{cald} = 1.751\ g\,cm^{-3}$, $\mu = 0.795\ mm^{-1}$, 93486 reflections collected, 8666 independent reflections, $wR$(all data) = 0.174, $R$(all data) = 0.167. CCDC 714016 (**1**-250 K), 714015 (**1**-110 K), 714014 (**1**-80 K) and 736427 (**1**-15 K) contain the supplementary crystallographic data for this paper. These data can be obtained free of charge from The Cambridge Crystallographic Data Centre via www.ccdc.cam.ac.uk/data_request/cif.

[15] Because symmetry breaking results in the monoclinic INT phase, the nonconventional space group $P22_12_1$ was chosen for the HS phase in order to retain the monoclinic $b$ axis.

[16] The INT phase is associated with an order/disorder, which would require treating the structures as the weighted contribution of HS and LS states on each independent site. However, due to the limited spatial resolution of the experiments, (ca. 0.8 Å) this disorder can not be solved, because the atomic displacements between HS and LS states are small (0.2 Å). The resulting pseudosymmetry yields high correlations in the refinements through nonpositive-definite thermal parameters in the structures with multiplied cell (INT, LS, and PIHS). The weak new reflections as well as the decrease in crystalline quality resulting from phase transitions may be at the origin of the $R$ factors. Internal $R$ factors are 0.053 (LS), 0.037 (INT), 0.030 (HS), and 0.140(PIHS).

[17] M. Nishino, K. Boukheddaden, S. Miyashita, F. Varret, *Phys. Rev. B* **2003**, *68*, 224402.

[18] D. Chernyshov, H.-B. Bürgi, M. Hostettler, K. W. Törnroos, *Phys. Rev. B* **2004**, *70*, 094116.

[19] F. H. Herbstein, *Acta Crystallogr. Sect. B* **2006**, *62*, 341 – 383.